Title
Evaluating the relative air permeability of porous media from their water retention curves

Journal
Water Resources Research, 52(5)

ISSN
0043-1397

Authors
Assouline, S
Tuli, A
Hopmans, JW

Publication Date
2016-05-01

DOI
10.1002/2015wr018286

AGU PUBLICATIONS

Water Resources Research

RESEARCH ARTICLE

10.1002/2015WR018286

Key Points:

- Relative air permeability is predicted using pore size distribution attributes
- Power value in the model is related to the coefficient of variation of the pore size distribution
- Proposed model provided accurate prediction of the soil RAP

Correspondence to:
S. Assouline,
vwshmuel@agri.gov.il

Citation:
Assouline, S., A. Tuli, and J. W. Hopmans (2016), Evaluating the relative air permeability of porous media from their water retention curves, *Water Resour. Res.*, *52*, 3428–3439, doi:10.1002/2015WR018286.

Received 25 OCT 2015
Accepted 7 MAR 2016
Accepted article online 12 MAR 2016
Published online 7 MAY 2016

Evaluating the relative air permeability of porous media from their water retention curves

S. Assouline[1], A. Tuli[2], and J. W. Hopmans[3]

[1]Institute of Soil, Water and Environmental Sciences, A.R.O.—Volcani Center, Bet Dagan, Israel, [2]California Environmental Protection Agency, Department of Pesticide Regulation, Environmental Monitoring Branch, Sacramento, California, USA, [3]Hydrology, Department of LAWR, University of California, Davis, California, USA

Abstract Accurate modeling of water and air flow in porous media requires the definition of the relevant hydraulic properties, namely, the water retention curve (WRC) and the relative hydraulic conductivity function (RHC), as well as the definition of the relative air permeability function (RAP). Capitalizing on the approach developed previously to represent the RHC, a new model allowing the prediction of RAP based on information resulting from the WRC is proposed. The power value η_a in the model is a decreasing exponential function of the coefficient of variation, ε, characterizing the pore size distribution of the porous medium, and derived from its WRC. The model was calibrated using data from 22 disturbed and undisturbed soil samples and was validated using data from eight soil types ranging from quartz sand to silty clay loam. The proposed model provided accurate prediction of the soil RAP and performed in some cases (sandy loam and silty clay loam soils) better than available alternative models.

1. Introduction

The need for accurate modeling of multiphase flow and transport processes is steadily increasing in various domains such as agriculture, hydrology, petroleum engineering, and environment-related issues such as groundwater remediation [*Honarpour et al*., 1986; *Stonestrom and Rubin*, 1989; *Springer et al*., 1995; *Clayton*, 1999; *Dury et al*., 1999; *Bhattarai et al*., 2006; *Niu et al*., 2012; *Ben Noah and Friedman*, 2015].

We will focus in the following on unsaturated flow conditions where water and air flow are involved, as the data being used correspond to experiments using air and water. However, the approach presented herein could in principle be applied to systems containing any wetting and nonwetting fluids.

Appropriate modeling of water movement in soils requires the definition of the relevant hydraulic properties, namely, the water retention curve (WRC) and the hydraulic conductivity function. Several modeling approaches and expressions were developed during the last century and a recent review can be found in *Assouline and Or* [2013]. Similarly, modeling the air movement in unsaturated porous media requires the definition of the air permeability as a function of water content [*Springer et al*., 1995].

In porous media, both air and water permeabilities are strong nonlinear functions of the respective phase contents [*Fischer et al*., 1997; *Moldrup et al*., 1998; *Selker et al*., 2007]. Often, these permeabilities are expressed relatively to the maximum value corresponding to the case where the pore space is fully saturated with the relevant phase, leading to the definition of the relative hydraulic conductivity function (RHC) or the relative air permeability function (RAP).

Concepts similar to the ones developed to describe the RHC were applied to express the RAP: *Clayton* [1999] applied the models of *Brooks and Corey* [1964] for the WRC and the RHC; *Tuli and Hopmans* [2004] applied the model of *Kosugi* [1996] for the WRC and the model of *Mualem* [1976] for the RHC; *Kuang and Jiao* [2011] applied the model of *van Genuchten* [1980] for the WRC and a variation based on the model of *Mualem* [1976] (with a power of 4 instead of the power of 2) for the RHC; *Yang and Mohanty* [2015] used the model of *Kosugi* [1996] for the WRC and compared the performances of the models of *Burdine* [1953], *Mualem* [1976], and *Alexander and Skaggs* [1986] for the RHC. The common main element in these different approaches is the transformation from the water content, θ_w, to the air content, θ_a, and it is often assumed that if S_{ew} denotes the effective water saturation, then the effective air saturation, S_{ea}, is equal to $(1 - S_{ew})$

10.1002/2015WR018286

[*Clayton*, 1999; *Tuli and Hopmans*, 2004; *Kuang and Jiao*, 2011; *Yang and Mohanty*, 2015] (S_{ew} and $S_{ea,}$ are defined below in equations (5) and (6)).

The movement of water and air in a porous medium is strongly affected by the attributes of the pore space represented generally in terms of pore size distribution, connectivity, and tortuosity [*Brooks and Corey*, 1964; *Brutsaert*, 1966; *Mualem*, 1976; *Kosugi*, 1996; *Moldrup et al.*, 2001; *Assouline*, 2001]. Several studies have addressed this issue in terms of pore network modeling and percolation theory and critical path analysis [*Fatt*, 1956a,b,c; *Jerauld and Salter*, 1990; *Heiba et al.*, 1992; *Hunt*, 2005a,b; *Hunt and Ewing*, 2009; *Ghanbarian-Alavijeh and Hunt*, 2012]. The WRC is strongly related to the pore size distribution [*Arya and Paris*, 1981; *Fredlund*, 2002]. The model for the WRC that has been proposed by *Assouline et al.* [1998] allows defining a parameter ε, the coefficient of variation of the pore size distribution derived from the WRC, which is a characteristic of the pore space that addresses both its mean and variance. This parameter was found to be correlated to the parameter λ in the WRC model of *Brooks and Corey* [1964] [*Assouline*, 2005] and to the parameter σ used in the WRC model of *Kosugi* [1996] [*Nasta et al.*, 2013; *Assouline and Or*, 2013]. The parameter ε was also strongly correlated to the power η that lumps the effects of connectivity and tortuosity on the RHC in the model of *Assouline* [2001] [*Assouline*, 2005; *Assouline and Or*, 2013]. The resulting $\eta(\varepsilon)$ relationship remained valid even when the WRC of compacted soil samples were considered [*Assouline*, 2006a]. The $\eta(\varepsilon)$ relationship expresses the strong link between the WRC and the RHC and allows predicting the RHC based on information on the pore space attributes of the medium under interest that are derived from the WRC. It should be interesting and of high practical value to check if a similar approach could also be applied to characterize the link between the WRC and the RAP.

The main objectives of this study are (i) to investigate the relationship between the WRC and the RAP stemming from the models of *Assouline et al*. [1998] for the WRC and *Assouline* [2001] for the RHC and (ii) to propose a model capable of predicting the RAP of porous media based on information available from their WRC.

2. Theoretical Aspects

The following model is applied herein to represent the WRC (see details in *Assouline et al*. [1998]):

$$S_{ew}(\psi)=1-\exp\left[-\xi_w\left(|\psi|^{-1}-|\psi_L|^{-1}\right)^{\mu_w}\right] \quad ; \quad 0 \le |\psi| \le |\psi_L| \tag{1}$$

where S_{ew} if the effective water saturation, ψ is the capillary head, ξ_w and μ_w are two fitting parameters, and ψ_L is the capillary head corresponding to a very low water content, θ_L, which represents the limit of interest for a particular WRC application (if no measured information on ψ_L and θ_L are available, ψ_L can be considered equal to 15 bars and θ_L set to correspond to θ_r). The advantage of this model is that the quantitative description of the WRC in equation (1) is also the probability function, $F(|\psi^{-1}|)=S_{ew}(|\psi^{-1}|)$, corresponding to the probability density function, *f*(*r*), representing the distribution of the pore radii, *r*, in the porous medium under interest since *r* is proportional to $|\psi|^{-1}$ [*Assouline et al.*, 1998; *Assouline*, 2006b]. The distribution *f*(*r*) can be characterized by the parameter ε representing the coefficient of variation of the distribution and defined as [*Assouline*, 2001, 2006b]:

$$\varepsilon=\frac{\left[\Gamma(1+2/\mu_w)-\Gamma^2(1+1/\mu_w)\right]^{0.5}}{\Gamma(1+1/\mu_w)+1/|\psi_L|} \tag{2}$$

where Γ is notation of the Gamma function.

Based on the relationship between the WRC and *f*(*r*), and applying the approach of *Mualem* [1976], a model for the RHC, $K_{rw}(S_{ew})$, was proposed by *Assouline* [2001]:

$$K_{rw}(S_{ew})=\left[\frac{\int_0^{S_{ew}}\frac{dF}{\psi}}{\int_0^1\frac{dF}{\psi}}\right]^{\eta_w} \tag{3}$$

where η_w is a parameter that is related to the soil texture and structure. The parameter η_w was found to be related to ε [*Assouline*, 2005]:

$$\eta_w = 1.10\,\varepsilon^{-0.624} \quad (r^2 = 0.88) \tag{4}$$

Analytical expressions of $K_{rw}(S_{ew})$ are available that depend on the applied model for the WRC [*Assouline and Tartakovsky*, 2001; *Assouline and Or*, 2013].

For a soil volume containing both air and water, the effective water saturation, S_{ew}, is defined as:

$$S_{ew} = \left(\frac{\theta_w - \theta_{rw}}{\theta_{sw} - \theta_{rw}} \right) \tag{5}$$

where θ_w is the volumetric water content, and θ_{sw} and θ_{rw} are the saturated and the residual water content, respectively. Similarly, the effective air saturation, S_{ea}, is defined as:

$$S_{ea} = \left(\frac{\theta_a - \theta_{ra}}{\theta_{sa} - \theta_{ra}} \right) \tag{6}$$

where θ_a is the volumetric air content, and θ_{sa} and θ_{ra} are the maximum and the minimum volumetric air content, respectively.

The saturation water content, θ_{sw}, is often smaller than the soil porosity, n, as some air may remain entrapped in the saturated samples [*Rogowski*, 1971]. The residual water content, θ_{rw}, is also difficult to determine and predict and some approaches were proposed [*Tuller and Or*, 2005]. Similar limitations apply to the definition and the prediction of θ_{sa} and θ_{ra}. Within the practical range of capillary tensions generally determining the WRC (up to 15 bars), the maximum volumetric air content, θ_{sa}, is smaller than the soil porosity, n, because of θ_{rw}. The minimum volumetric air content, θ_{ra}, can be in some cases equal to zero, as assumed by *Millington and Quirk* [1960], but it is generally greater than zero as it stems from continuum percolation theory [*Hunt*, 2004, 2005a]. *Ghanbarian-Alavijeh and Hunt* [2012] showed that θ_{ra} could be predicted by $(n - \theta_{sw})$. Relying on the above considerations, the following relationships could be set:

$$\theta_a = n - \theta_w \tag{7a}$$

$$\theta_{sa} = n - \theta_{rw} \tag{7b}$$

$$\theta_{ra} = n - \theta_{sw} \tag{7c}$$

Replacing equation (7) with equation (6) leads to:

$$S_{ea} = (1 - S_{ew}) \tag{8}$$

Consequently, the conditions on the RAP, K_{ra}, are:

$$\begin{aligned} K_{ra} &= 0 \quad ; \quad S_{ea} = 0 \\ K_{ra} &= 1 \quad ; \quad S_{ea} = 1 \end{aligned} \tag{9}$$

Based on equation (8), the RHC model in equation (3) can be, in principle, applied to define the RAP. However, since the interaction between the air and the pore space attributes like pore size distribution, connectivity, and tortuosity is different from that of the water, the power η_a is expected to differ from η_w:

$$K_{ra}(S_{ea}) = \frac{K_a(S_{ea})}{K_{sa}} = \left[\frac{\int_0^{S_{ea}} \frac{dF}{\psi}}{\int_0^1 \frac{dF}{\psi}} \right]^{\eta_a} \tag{10}$$

with $K_a(S_{ea})$ being the air permeability at a given S_{ea} value, and K_{sa}, the saturated air permeability corresponding to $S_{ea} = 1.0$. Applying this approach to a wide range of soil types characterized by different specific ε values, the resulting $\eta_a(\varepsilon)$ relationship could be determined and investigated.

3. Methodology

Experimental data on WRC and $K_a(S_{ew})$ functions for a relatively large range of soil types are used to establish and validate the proposed approach. These data were presented previously in different studies where

Table 1. The Soil Samples Used to Calibrate and Validate the Proposed RAP Model and the Corresponding Values of ε, Fitted η_a, and Predicted η_a According to Equation (12)

Soil Type	ε	η_a—Best Fit	η_a—Equation (12)	Reference
Calibration				
Volcanic sand	0.288	1.75	2.01	*Brooks and Corey* [1964]
Fine sand	0.268	2.00	2.06	
Touchet silt loam	0.359	1.67	1.85	
Glass beads	0.100	2.80	2.49	
D44	1.378	0.90	0.58	*Tuli et al.* [2005]—Disturbed samples
D59	1.012	0.62	0.88	
D126	1.220	0.55	0.69	
D128	1.085	1.10	0.81	
D129	1.122	0.92	0.77	
D132	0.739	0.80	1.20	
D134	0.956	0.65	0.93	
D140	1.374	0.83	0.58	
D142	2.014	0.70	0.28	
UD128	1.443	0.30	0.53	*Tuli et al.* [2005]—Undisturbed samples
UD129	1.413	0.50	0.55	
UD131	1.378	0.55	0.58	
UD134	1.621	0.35	0.44	
UD137	1.575	0.60	0.46	
UD138	2.906	0.20	0.10	
UD139	2.168	0.33	0.23	
UD140	2.164	0.31	0.23	
UD142	3.296	0.13	0.06	
Validation				
Columbia sandy loam	1.434	0.70	0.54	*Tuli and Hopmans* [2004]
Oso Flaco sand	0.277	1.57	2.04	
Hygiene sandstone	0.206	2.20	2.21	*Brooks and Corey* [1964]
Amarillo silty clay loam	0.666	1.35	1.30	
Mixed sand	0.287	2.30	2.01	*Dury et al.* [1999]
Oakley sand	0.272	2.40	2.05	*Stonestrom and Rubin* [1989]
Grenoble sand	0.801	0.91	1.11	*Touma and Vauclin* [1986]
Quartz sand	0.353	1.90	1.87	*Fischer et al.* [1997]

more details on the measuring methods are available (Table 1). Most of the data were used to establish the resulting $\eta_a(\varepsilon)$ relationship while the remaining part was used to provide a preliminary validation of that relationship (Table 1).

The available data consisted in general in a series of measured $\theta_w(\psi)$ values with their corresponding $K_a(\theta_w)$ values. Using the respective reported saturated and residual water contents, θ_{sw} and θ_{rw}, of the different soil samples, $\theta_w(\psi)$ was expressed in terms of $S_{ew}(\psi)$. In the data set from *Tuli et al.* [2005], θ_{rw} values were not reported. These were estimated by first using the respective clay fractions of each soil to compute their specific surface areas following *Or and Wraith* [1999], and then by applying the method of *Tuller and Or* [2005] to estimate the corresponding θ_{rw} for a film thickness at a tension of 15 bars. For each soil, equation (1) was fitted to the measured $S_{ew}(\psi)$ data, and the corresponding parameters ξ_w and μ_w were determined. The respective ε values were then computed using equation (2). In addition, for each soil, it was possible to express the measured $K_a(\theta_w)$ values in terms of $K_a(S_{ea})$ using equation (8). In the data set from *Tuli et al.* [2005], the K_{sa} values in equation (10) were not reported. These were estimated by fitting the following power function [*Tuli and Hopmans*, 2004] to the measured $K_a(S_{ea})$ data:

$$K_a(S_{ea})=K_{sa}S_{ea}{}^{\gamma} \tag{11}$$

where K_{sa} and γ are fitting parameters. Consequently, some soil samples presented in *Tuli et al.* [2005] were not considered as it was not possible to achieve a reliable estimate of K_{sa} using this method (mostly cases where the maximal available measured K_a value was $\sim$10% of the estimated K_{sa}). It was then possible to compute $K_{ra}(S_{ea})$ according to equation (10) and to determine η_a for each soil sample from the best fit between the respective computed and measured $K_{ra}(S_{ea})$ values. The data from *Tuli et al.* [2005], involving both disturbed and undisturbed soil samples, and part of the data from *Brooks and Corey* [1964] (4 out of the 6 soils) were used to determine the $\eta_a(\varepsilon)$ relationships, and technically calibrate the proposed $K_{ra}(S_{ea})$ model. The remaining part of the data from *Brooks and Corey* [1964] and the data from *Tuli and Hopmans* [2004], *Dury*

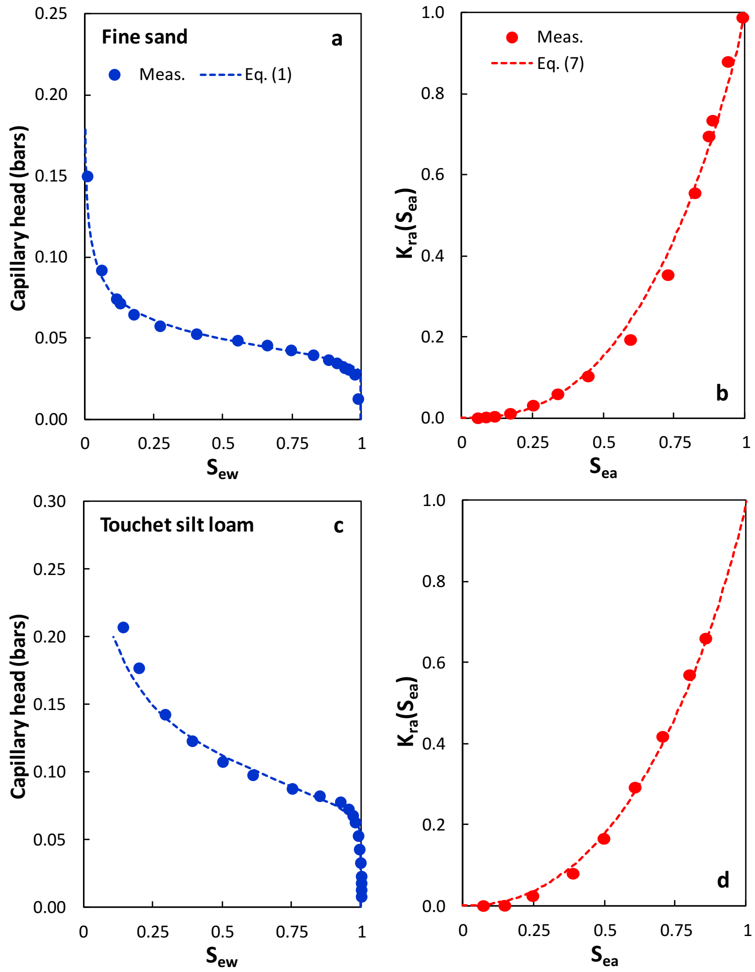

Figure 1. The fitted (a and c) WRC (equation (1)) and (b and d) RAP (equation (10)) to the measured $S_{ew}(\psi)$ (blue) and $K_{ra}(S_{ea})$ (red) data points for the Fine sand and the Touchet silt loam soils.

et al. [1999], *Stonestrom and Rubin* [1989], *Touma and Vauclin* [1986], and *Fischer et al.* [1997] were used to validate the proposed model and to evaluate its predictive ability with the previously estimated $\eta_a(\varepsilon)$ relationships. The calibration of the model relied on 22 soil samples while its validation relied on 8 soil types covering a wide range of porous media, from quartz sand to silty clay loam soil.

4. Results

The results in terms of the calculated ε and the fitted η_a values are presented in Table 1 for each soil type. The fitted equation (1) and equation (10) to the data for the Fine sand and the Touchet silt loam are illustrated in Figures 1a and 1d. The model in equation (1) reproduces accurately the specific $S_{ew}(\psi)$ function for each soil, including the sharp transition at the vicinity of the air entry value for the sand (Figure 1a), as previously reported [*Assouline et al.*, 1998]. Similarly, the RAP model in equation (10) provides a good representation of the measured $K_{ra}(S_{ea})$ data points (Figures 1b and 1d).

The resulting $\eta_a(\varepsilon)$ relationship characterizing the data set in Table 1 is depicted in Figure 2. A clear exponentially decreasing function characterizes this relationship, as it was the case for the $\eta_w(\varepsilon)$ relationship [*Assouline*, 2001, 2005]. Using only the data set for calibration (Table 1; full circles in Figure 2), the following expression was fitted to the data points:

$$\eta_a = 2.80\, e^{-1.15\varepsilon} \quad (r^2 = 0.89) \tag{12}$$

The summary of the statistical significance of the estimated parameters is provided in Table 2. It is interesting to note that the ε values corresponding to the undisturbed soil samples are higher than those corresponding to the disturbed ones, in agreement with the conclusion of *Tuli et al.* [2005] regarding the loss of soil structure in the disturbed samples.

The data points corresponding to the eight soil types from the validation data set (Table 1), with η_a being estimated based on ε using equation (12), are represented by the empty circles in Figure 2. They all fall within the 90% confidence level range of the calibrated curve (dashed curves). The predicted $K_{ra}(S_{ea})$ functions for these eight soil types are shown in Figure 3 against the corresponding measured data points. The root-mean-square deviation (*rmsd*) quantifying the level of agreement between the proposed model (equation (10)) and the experimental data is provided in Table 3a. Overall, the proposed model provides a relatively good prediction of the RAP. It is excellent in some cases, mainly for sands (Figures 3b and 3c), and fair in others, like in the

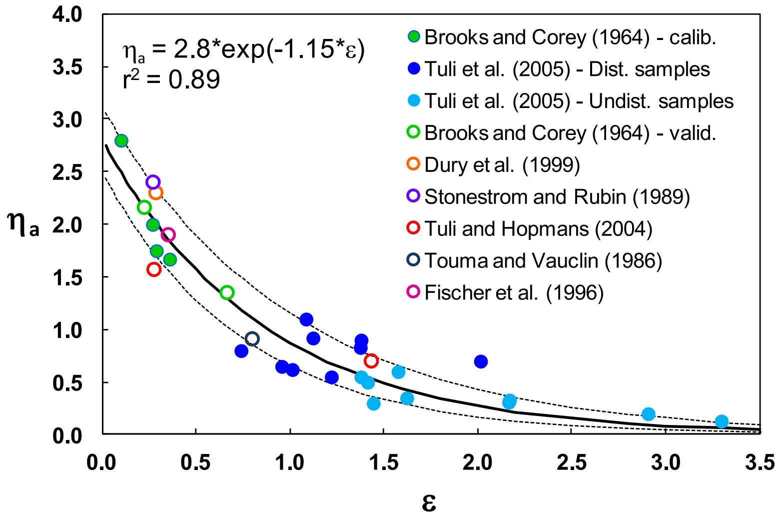

Figure 2. The $\eta_a(\varepsilon)$ points characterizing the data set in Table 1 and the fitted relationship (equation (12); black curve). Full circles correspond to the calibration data set and empty circles to the validation one. The dashed lines correspond to the $\pm$90% confidence intervals of the fitting parameters of equation (12) (Table 2).

case of the Columbia sandy loam (Figure 3a) where it seems that there is a discontinuity in the measured points around $S_{ea}=0.65$ that does not correspond to the monotonic and unimodal WRC [*Tuli and Hopmans*, 2004], indicating that some errors in permeability measurements are most probably involved for this specific soil sample.

The model of *Mualem* [1976] with the constant theoretical power of 2 and the correction factor ($S_{ea}{}^{0.5}$) was often considered capable to provide also a reliable expression of the $K_{ra}(S_{ew})$ function [*Tuli and Hopmans*, 2004; *Yang and Mohanty*, 2015];

$$K_{ra}(S_{ew})=(1-S_{ew})^{0.5}\left[\frac{\int_{S_{ew}}^{1}\frac{dS_{ew}}{\psi}}{\int_{0}^{1}\frac{dS_{ew}}{\psi}}\right]^2 \tag{13}$$

Applying the same model, *Kuang and Jiao* [2011] suggested that $K_{ra}(S_{ew})$ could be better estimated if the theoretical constant power of 2 of *Mualem* [1976] is replaced by an empirical constant value of 4:

Table 2. Statistical Significance of the Estimated Parameters of the Fitted Equations (12) and (17) to Air and Water Data in Figures 2 and 5a, and When a Unique Curve Is Fitted to All the Points in Figure 5a (the Two Outliers Excluded)

	r^2	r^2 (DF Adj)	Fit Std Error	F Value	
Equation (12)					
	0.890	0.878	0.233	161.168	
Parameters	Values	Std. Error	t value	90% confidence limits	
a	2.798	0.193	14.495	2.465	3.130
b	−1.148	0.105	−10.951	−1.329	−0.967
Equation (17)					
	0.872	0.855	0.277	108.780	
Parameters	Values	Std. Error	T value	90% confidence limits	
a	3.370	0.223	15.121	2.981	3.759
b	−0.994	0.134	−7.431	−1.227	−0.760
Unique Curve					
	0.875	0.867	0.311	266.873	
Parameters	Values	Std. Error	t value	90% confidence limits	
a	3.278	0.175	18.762	2.983	3.572
b	−1.131	0.096	−11.730	−1.294	0.969

$$K_{ra}(S_{ew})=(1-S_{ew})^{0.5}\left[\frac{\int_{S_{ew}}^{1}\frac{dS_{ew}}{\psi}}{\int_{0}^{1}\frac{dS_{ew}}{\psi}}\right]^{4} \tag{14}$$

The predictive capability of equations (13) and (14) is depicted also in Figure 3 along with that of the proposed model (equations (10) and (12)), and the corresponding *rmsd* values are presented in Table 3a. Equation (13) with the constant power of 2 presents the lowest performance, systematically overestimating the K_{ra} values, in agreement with the results of *Kuang and Jiao* [2011]. It is clear that replacing the constant power of 2 by the value of 4, as suggested by *Kuang and Jiao* [2011], improves significantly the predictive ability of the model. However, it seems, at least from this validation data set, that equation (14) on the overall performs better than equation (13), which fails to represent soils containing a clay component (Table 3a). The main advantage of the proposed model in equation (10) that links η_a to ε, as it successfully linked η_w to ε [*Assouline*, 2001, 2005], is that it is flexible enough to correspond accurately to a wide variety of soil types since it releases the constraint of using a constant value for the power in equations (13) and (14).

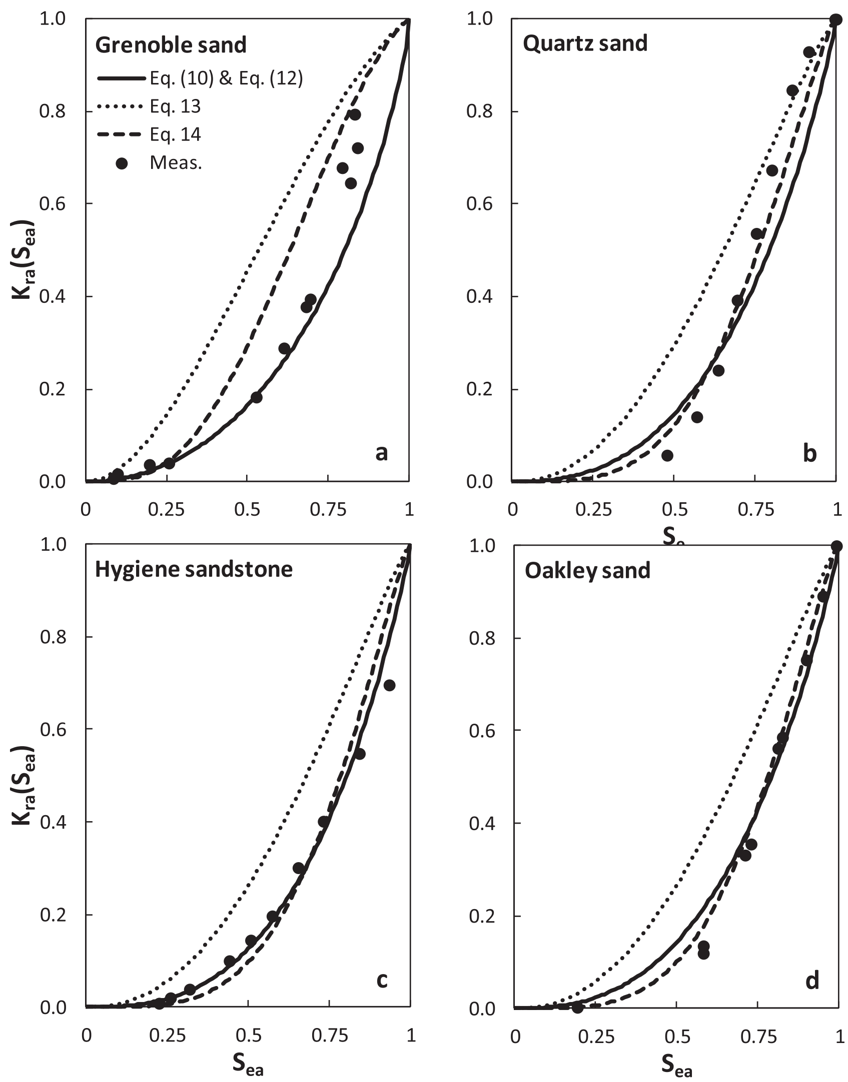

Figure 3. The predicted $K_{ra}(S_{ea})$ functions for the soil samples in the validation data set according to the proposed model (equations (10) and (12)) and following equations (13) and (14) versus the corresponding measured data points.

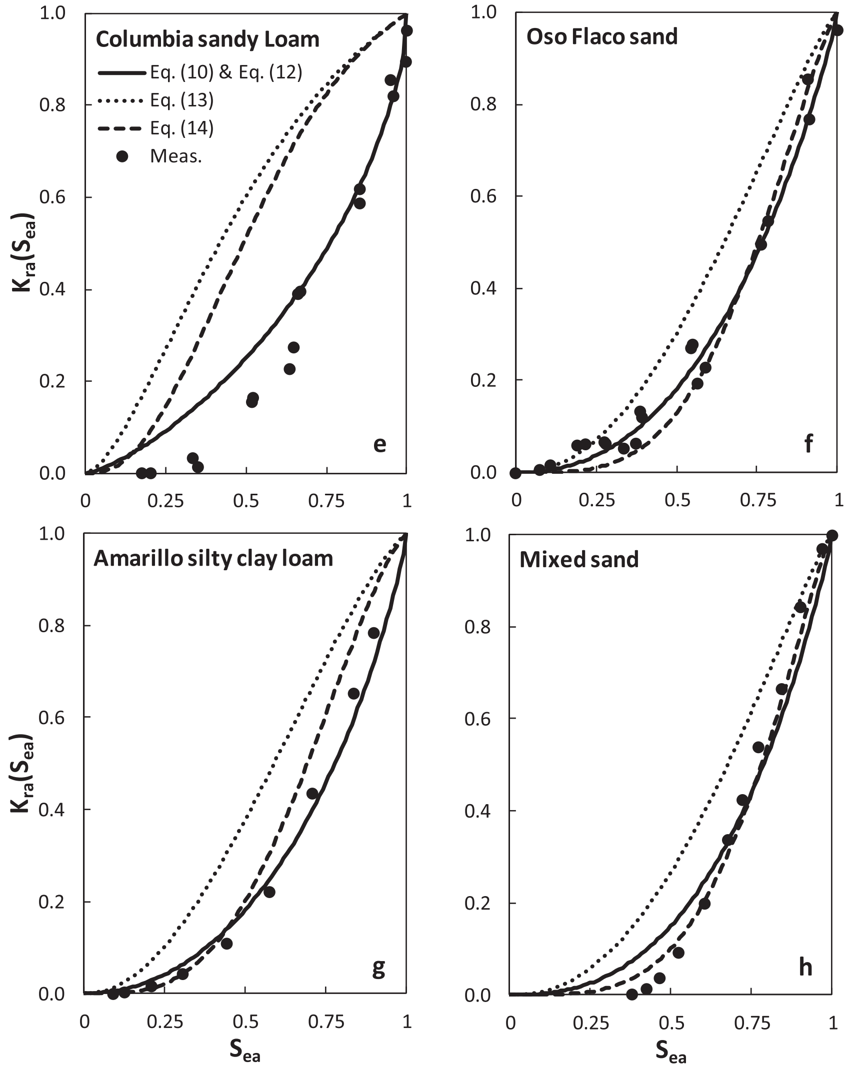

Figure 3. (continued)

Millington and Quirk [1960] has proposed the following model for the relative air permeability of porous media, K_{ra}, assuming $\theta_{ra}=0$:

$$K_{ra}=\left(\frac{\theta_a}{n}\right)^2 \tag{15}$$

Table 3a. The Root-Mean-Square Deviation (*rmsd*) of the Models in Equations (10), (13), and (14) From the Experimental Data for the Soils in the Validation Data Set (Figure 3)

Soil	Equation (10)	Equation (13)	Equation (14)
Columbia sandy loam	0.081	0.338	0.381
Oso Flaco sand	0.034	0.094	0.048
Hygiene sandstone	0.032	0.140	0.059
Amarillo silty clay loam	0.033	0.156	0.064
Mixed sand	0.066	0.133	0.038
Oakley sand	0.049	0.165	0.028
Grenoble sand	0.105	0.196	0.119
Quartz sand	0.099	0.126	0.057

Ghanbarian-Alavijeh and Hunt [2012] released the assumption of $\theta_{ra}=0$ and suggested that:

$$K_{ra}=\left(\frac{\theta_a-\theta_{ra}}{n-\theta_{ra}}\right)^2 \tag{16}$$

where θ_{ra} is defined according to equation (7c). It is interesting to note that, in equation (16), $\theta_{sa}=n$, which is equivalent to the assumption that

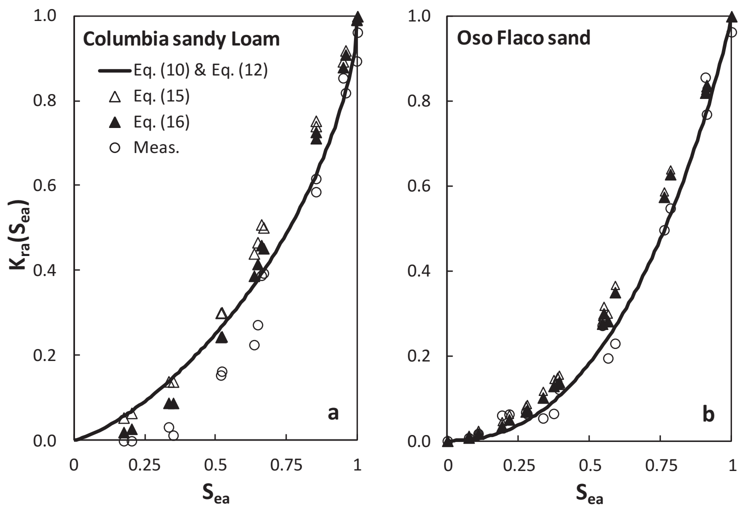

Figure 4. The predicted $K_{ra}(S_{ea})$ functions for the soil samples in the data set of *Tuli and Hopmans* [2004] according to the proposed model (equations (10) and (12)) and following equations (15) and (16) versus the corresponding measured data points.

$\theta_{rw} = 0$, which is unlikely to characterize porous media. These two models were applied to the two soils from the data set of *Tuli and Hopmans* [2004] for which all the required variables were available. The results from these two models are depicted in Figure 4, along with the curve predicted by the proposed model, and the corresponding *rmsd* values presented in Table 3b. Accounting for θ_{ra} according to equation (7c) [*Ghanbarian-Alavijeh and Hunt*, 2012] slightly improve the performances of the Millington and Quirk model (equation (15)) but the overall best fit corresponds to the proposed model in equations (10) and (12) (Table 3b), even for the problematic data of the Columbia sandy loam. Considering θ_{ra} as a fitting parameter [*Ghanbarian-Alavijeh and Hunt*, 2012] improves the fit to the experimental data but such an approach is devoid of any predictive capability.

The empirical power function that was fitted to the (ε, η_w) data (equation (4)) inherently assumes that $\eta_w \rightarrow +\infty$ when $\varepsilon \rightarrow 0$. Physically speaking, $\varepsilon = 0$ corresponds to a porous medium characterized by a unique pore radius and, therefore, η_w, should tend toward a finite value rather than to $+\infty$ when $\varepsilon \rightarrow 0$. In that sense, the exponential function (equation (12)) fitted to the (ε, η_a) data is more appropriate as it allows the power η to have a finite value for $\varepsilon = 0$. A similar exponential function to equation (12) was fitted to the (ε, η_w) data used to determine equation (4). The resulting fitted expression is:

$$\eta_w = 3.37\, e^{-0.99\,\varepsilon} \quad (r^2 = 0.87) \tag{17}$$

The statistical significance of its estimated parameters is also provided in Table 2. The curves corresponding to the expressions $\eta_a(\varepsilon)$ (equation (12)) and $\eta_w(\varepsilon)$ (equation (17)), that were fitted to the respective (ε, η_a) and (ε, η_w) data points, are depicted in Figure 5a. For any given ε, the η_w values are systematically higher than the η_a values. One could argue that since there is some overlap in the 90% confidence intervals of the fitted parameters of equations (12) and (17), they might not be statistically different, and all the points depicted in Figure 5a could have been considered as one single sample, meaning that there is no difference between η_a and η_w for a given ε. The resulting parameters for a unique expression of the type of equation (12) or (17) corresponding to such an assumption are given in Table 2. From a physical point of view, such assumption could correspond to the simplest conceptual representation of a porous medium, namely, an assembly of parallel cylindrical capillaries with no connections between them [*Purcell*, 1949; *Fatt and Dykstra*, 1951]. In such case, one could assume that only minor differences (resulting from impurities and roughness in the capillary walls for example) could characterize the air and water permeabilities and that, from any practical aspect, η could be considered unique for air and water. However, more complex conceptual models of the porous medium could be considered: interconnections between the capillaries [*Childs and Collis-George*, 1950]; angular pores allowing simultaneous presence of air and water within the same pore [*Dullien et al.*, 1986; *Or and Tuller*, 2000; *Tuller and Or*, 2001]; polydisperse and lognormally distributed spheres rather than capillaries [*Chan and Govindaraju*, 2003, 2004]. In such cases, it is likely that the permeability for air and that for water will differ because of the different paths that water and air could use to move in the resulting network of

Table 3b. The Root-Mean-Square Deviation (*rmsd*) of the Models in Equations (10), (15), and (16) From the Experimental Data for Two Soils in the Data Set of *Tuli and Hopmans* [2004] (Figure 4)

Soil	Equation (10)	Equation (15)	Equation (16)
Columbia sandy loam	0.081	0.125	0.089
Oso Flaco sand	0.034	0.057	0.049

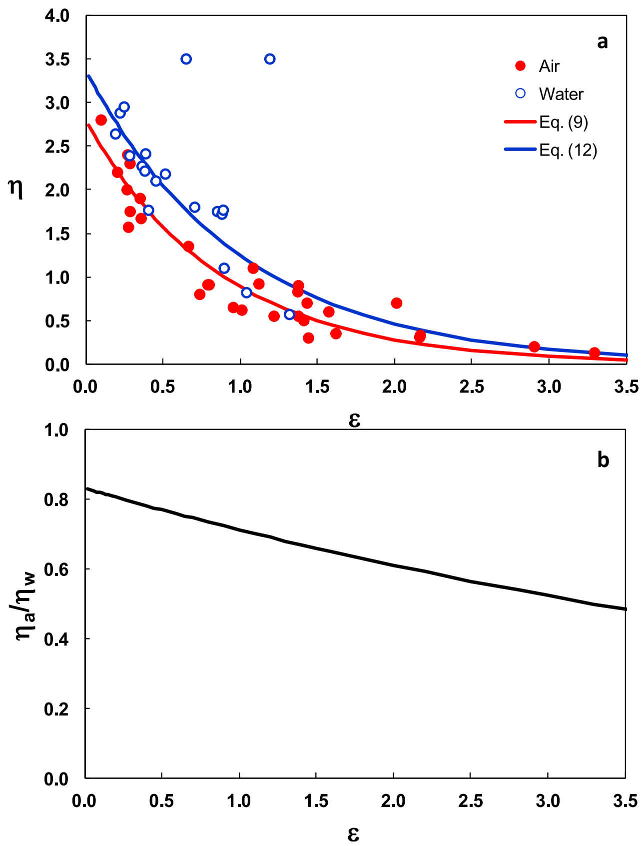

Figure 5. (a) The expressions $\eta_a(\varepsilon)$ (equation (12); red curve) and $\eta_w(\varepsilon)$ (equation (17); blue curve) fitted to the respective (ε, η_a) and (ε, η_w) data points (the two outliers excluded); (b) the relationship between the ratio (η_a/η_w) and ε.

interconnected pores or voids. This is supported by the results from the application of continuum percolation theory [*Sahimi*, 2011; *Hunt*, 2005b; *Hunt and Ewing*, 2009]. Since the η value in equation (3) or equation (10) represents the lumped impact of pore connectivity and tortuosity on the hydraulic or the air permeability [*Assouline*, 2001], it is conceivable that a specific η value will characterize each phase. Moreover, the result in Figure 5a, suggesting that $\eta_w > \eta_a$ for any given ε, is in agreement with the findings of *Tuli et al.* [2005] and with the conclusion of *Moldrup et al.* [2001] that the liquid-phase tortuosity is typically equal or larger than the gaseous phase tortuosity. The ratio (η_a/η_w) decreases as ε increases (Figure 5b). As the coefficient of variation of the pore size distribution of the porous medium increases, the relative difference between the interactions of water and air with the pore space attributes like connectivity and tortuosity, increases, and consequently the relative difference between η_a and η_w increases.

5. Summary and Conclusions

A model allowing the prediction of the RAP based on information on the pore size distribution derived from the soil WRC has been presented. The model relies on the WRC model of *Assouline et al.* [1998] and applies the approach proposed in *Assouline* [2001] to define the corresponding soil RHC. Based on experimental data for a wide range of soil types, the proposed RAP model was calibrated and validated, providing accurate prediction of the soil RAP and performing in most cases better than available alternative models.

The application of the model involves the following steps:

1. Fit equation (1) to S_{ew} (ψ) based on available soil WRC data.
2. Compute the value of ε representing the coefficient of variation of the pore size distribution using equation (2).
3. Compute η_a according to equation (12).
4. Estimate the soil RAP, $K_{sa}(S_{ea})$, according to equation (10) and assuming equation (8).

Acknowledgment
Data sets are from literature cited in the manuscript, which are available upon request.

References

Alexander, L., and R. W. Skaggs (1986), Predicting unsaturated hydraulic conductivity from the soil water characteristic, *Trans. Am. Soc. Agric. Eng.*, *29*(1), 176–184.
Assouline, S. (2001), A model for soil relative hydraulic conductivity based on the water retention characteristic curve, *Water Resour. Res.*, *37*(2), 265–271.
Assouline, S. (2005), On the relationships between the pore size distribution index and characteristics of the soil hydraulic functions, *Water Resour. Res.*, *41*, W07019, doi:10.1029/2004WR003511.
Assouline, S. (2006a), Modeling the relationship between soil bulk density and the hydraulic conductivity function, *Vadose Zone J.*, *5*, 697–705.
Assouline, S. (2006b), Modeling the relationship between soil bulk density and the water retention curve, *Vadose Zone J.*, *5*, 554–563.
Assouline, S., and D. Or (2013), Conceptual and parametric representation of soil hydraulic properties: A review, *Vadose Zone J.*, *12*, 1–20, doi:10.2136/vzj2013.07.0121.
Assouline, S., and D. Tartakovsky (2001), Unsaturated hydraulic conductivity function based on a fragmentation process, *Water Resour. Res.*, *37*(5), 1309–1312, doi:10.1029/2000WR900332.

Assouline, S., D. Tessier, and A. Bruand (1998), A conceptual model of the soil water retention curve, *Water Resour. Res.*, *34*(2), 223–231.

Arya, L. M., and J. F. Paris (1981), A physicoempirical model to predict the soil moisture characteristic from particle-size distribution and bulk density data, *Soil Sci. Soc. Am. J.*, *45*, 1023–1030.

Ben Noah, I., and S. P. Friedman (2015), Continuum modeling of steady air injection into partially saturated soils, *Vadose Zone J.*, *14*(9), 16, doi:10.2136/vzj2014.12.0170.

Bhattarai, S. P., L. Pendergast, and D. J. Midmore (2006), Aeration improves yield and water use efficiency of irrigated tomato in heavy clay and saline soils, *Sci. Horticulturae*, *108*, 278–288, doi:10.1016/j.scienta.2006.02.011.

Brooks, R. H., and A. T. Corey (1964), Hydraulic properties of porous media, *Hydrol. Pap. 3*, pp. 1–27, Colo. State Univ., Fort Collins.

Brutsaert, W. (1966), Probability laws for pore-size distributions, *Soil Sci.*, *101*(2), 85–92.

Burdine, N. T. (1953), Relative permeability calculations from pore size distribution data, *J. Pet. Technol.*, *5*(3), 71–78, doi:10.2118/225-G.

Chan, T. P., and R. S. Govindaraju, (2003), A new model for soil hydraulic properties based on a stochastic conceptualization of porous media, *Water Resour. Res.*, *39*(7), 1195, doi:10.1029/2002WR001954.

Chan, T. P., and R. S. Govindaraju (2004), Estimating soil water retention curve from particle-size distribution data based on polydisperse sphere systems, *Vadose Zone J.*, *3*, 1443–1454.

Childs, E. C., and G. N. Collis-George (1950), The permeability of porous materials, *Proc. R. Soc. London, Ser. A*, *201*, 392–405.

Clayton, W. S. (1999), Effects of pore scale dead-end air fingers on relative permeabilities for air sparging in soils, *Water Resour. Res.*, *35*, 2909–2919, doi:10.1029/1999WR900202.

Dullien, F. A. L., F. S. Y. Lai, and I. F. Macdonald (1986), Hydraulic continuity of residual wetting phase in porous media, *J. Colloid Interface Sci.*, *109*, 201–218.

Dury, O., U. Fischer, and R. Schulin (1999), A comparison of relative nonwetting-phase permeability models, *Water Resour. Res.*, *35*(5), 1481–1493, doi:10.1029/1999WR900019.

Fatt, I. (1956a), The network model of porous media i: Capillary pressure characteristics, *Trans. Am. Inst. Min. Metall. Pet. Eng.*, *207*, 144–159.

Fatt, I. (1956b), The network model of porous media ii: Dynamic properties of a single size tube network, *Trans. Am. Inst. Min. Metall. Pet. Eng.*, *207*, 160–163.

Fatt, I. (1956c), The network model of porous media iii: Dynamic properties of network with tube radius distribution, *Trans. Am. Inst. Min. Metall. Pet. Eng.*, *207*, 164–181.

Fatt, I., and H. Dykstra (1951), Relative permeability studies, *J. Pet. Technol.*, *3*, 249–255.

Fischer, U., O. Dury, H. Flühler, and M. T. van Genuchten (1997), Modeling nonwetting-phase relative permeability accounting for a discontinuous nonwetting phase, *Soil Sci. Soc. Am. J.*, *61*(5), 1348–1354, doi:10.2136/sssaj1997.03615995006100050009x.

Fredlund (2002), Use of the grain-size distribution for estimation of the soil-water characteristic curve, *Can. Geotech. J.*, *39*, 1103–1117, doi:10.1139/t02-049.

Ghanbarian-Alavijeh, B., and A. G. Hunt (2012), Comparison of the predictions of universal scaling of the saturation dependence of the air permeability with experiment, *Water Resour. Res.*, *48*, W08513, doi:10.1029/2011WR011758.

Heiba, A. A., M. Sahimi, L. E. Scriven, and H. T. Davis (1992), Percolation theory of two-phase relative permeability, *SPE Form Eval.*, *7*, 123–132.

Honarpour, M. M., L. Koederitz, and A. H. Harvey (1986), *Relative Permeability of Petroleum Reservoirs*, CRC Press, Boca Raton, Fla.

Hunt, A. G. (2004), Continuum percolation theory for water retention and hydraulic conductivity of fractal soils: 1. Estimation of the critical volume fraction for percolation, *Adv. Water Resour.*, *27*, 175–183.

Hunt, A. G. (2005a), Continuum percolation theory for saturation dependence of air permeability, *Vadose Zone J.*, *4*, 134–138, doi:10.2113/4.1.134.

Hunt, A. G. (2005b), *Percolation Theory for Flow in Porous Media, Lect. Notes Phys.*, vol. 674, Springer, Berlin.

Hunt, A. G., and R. P. Ewing (2009), *Percolation Theory for Flow in Porous Media, Lect. Notes Phys.*, vol. 771, 2nd ed., Springer, Berlin.

Jerauld, G. R., and S. J. Salter (1990), The effect of pore-structure on hysteresis in relative permeability and capillary pressure: Pore level modeling, *Transp. Porous Media*, *5*, 103–151.

Kosugi, K. (1996), Lognormal distribution model for unsaturated soil hydraulic properties, *Water Resour. Res.*, *32*(9), 2697–2703, doi:10.1029/96WR01776.

Kuang, X., and J. J. Jiao (2011), A new model for predicting relative nonwetting phase permeability from soil water retention curves, *Water Resour. Res.*, *47*, W08520, doi:10.1029/2011WR010728.

Millington, R. J., and J. M. Quirk (1960), Transport in porous media, in *Transactions of 7th International Congress of Soil Science*, Madison, Wisc., U.S.A., vol. 1, edited by F. A. Van Beren et al., pp. 97–106, Elsevier, Amsterdam, Netherlands.

Moldrup, P., T. G. Poulsen, P. Schjønning, T. Olesen, and T. Yamaguchi (1998), Gas permeability in undisturbed soils: Measurements and predictive models, *Soil Sci.*, *163*, 180–189.

Moldrup, P., T. Olesen, T. Komatsu, P. Schjønning, and D. E. Rolston (2001), Tortuosity, diffusivity, and permeability in the soil liquid and gaseous phases, *Soil Sci. Soc. Am. J.*, *65*, 613–623, doi:10.2136/sssaj2001.653613x.

Mualem, Y. (1976), A new model for predicting the hydraulic conductivity of unsaturated porous media, *Water Resour. Res.*, *12*(3), 513–522, doi:10.1029/WR012i003p00513.

Nasta, P., S. Assouline, J. B. Gates, J. W. Hopmans, and N. Romano (2013), Prediction of unsaturated relative hydraulic conductivity from Kosugi's water retention function, *Proc. Environ. Sci.*, *19*, 609–617, doi:10.1016/j.proenv.2013.06.069.

Niu, W., Q. Guo, X. Zhou, and M. J. Helmers (2012), Effect of aeration and soil water redistribution on the air permeability under subsurface drip irrigation, *Soil Sci. Soc. Am. J.*, *76*, 815–820, doi:10.2136/sssaj2011.0329.

Or, D., and M. Tuller (2000), Flow in unsaturated fractured porous media: Hydraulic conductivity of rough surfaces, *Water Resour. Res.*, *36*(5), 1165–1177.

Or, D., and J. M. Wraith (1999), Temperature effects on soil bulk dielectric permittivity measured by time domain reflectometry: A physical model, *Water Resour. Res.*, *35*(2), 371–383.

Purcell, W. R. (1949), Capillary pressures—Their measurements using mercury and the calculation of permeability therefrom, *J. Pet. Technol.*, *1*, 39–48.

Rogowski, A. S. (1971), Watershed physics: Model of soil moisture characteristics, *Water Resour. Res.*, *7*(6), 1575–1582.

Sahimi, M. (2011), *Flow and Transport in Porous Media and Fractured Rock: From Classical Methods to Modern Approaches*, 709 pp., Wiley, Weinheim, Germany, doi:10.1002/9783527636693.

Selker, J. S., M. Niemet, N. G. McDuffie, S. M. Gorelick, and J.-Y. Parlange (2007), The local geometry of gas injection into saturated homogeneous porous media, *Transp. Porous Media*, *68*, 107–127, doi:10.1007/s11242-006-0005-0.

Springer, D. S., S. J. Cullen, and L. G. Everett (1995), Laboratory studies on air permeability, in *Handbook of Vadose Zone Characterization and Monitoring*, edited by L. G. Wilson, L. G. Everett, and S. J. Cullen, A. F. Lewis, Boca Raton, Fla.

Stonestrom, D. A., and J. Rubin (1989), Air permeability and trapped-air content in two soils, *Water Resour. Res.*, *25*(9), 1959–1969.
Touma, J., and M. Vauclin (1986), Experimental and numerical analysis of two-phase infiltration in a partially saturated soil, *Transp. Porous Media*, *1*, 27–55.
Tuli, A., and J. W. Hopmans (2004), Effect of degree of fluid saturation on transport coefficient in disturbed soils, *Eur. J. Soil Sci.*, *55*(1), 147–164, doi:10.1046/j.1365-2389.2003.00551.x.
Tuli, A., J. W. Hopmans, D. E. Rolston, and P. Moldrup (2005), Comparison of air and water permeability between disturbed and undisturbed soils, *Soil Sci. Soc. Am. J.*, *69*(5), 1361–1371, doi:10.2136/sssaj2004.0332.
Tuller, M., and D. Or (2001), Hydraulic conductivity of variably saturated porous media: Film and corner flow in angular pore space, *Water Resour. Res.*, *37*(5), 1257–1276.
Tuller, M., and D. Or (2005), Water films and scaling of soil characteristic curves at low water contents, *Water Resour. Res.*, *41*, W09403, doi:10.1029/2005WR004142.
van Genuchten, M. T. (1980), A closed-form equation for predicting the hydraulic conductivity of unsaturated soils, *Soil Sci. Soc. Am. J.*, *44*(5), 892–898, doi:10.2136/sssaj1980.03615995004400050002x.
Yang, Z., and B. P. Mohanty (2015), Effective parametrizations of three nonwetting phase relative permeability models, *Water Resour. Res.*, *51*, 6520–6531, doi:10.1002/2014WR016190.